Chapter 3

Electrochemical study of GSH-CDNB reaction in methanol and ethanol and the influence of GST and pesticides on it

3.1 Introduction

A brief introduction of glutathione S –transferase enzyme and its catalytic activities has already been covered in chapter 1. GSTs are a multigenic family of cytosolic proteins with multifunctional biological roles, widely distributed throughout the body and found in the liver, kidney, brain, pancreas, testis, heart, lung, small intestine, skeletal muscles, prostate and spleen [1]. Important biological function of GSTs is their catalytic action in detoxification reaction [2]. Over expressions of GST during phase II metabolism or the drug resistance associated with anticancer therapies of human [3,4] and the resistance acquired by certain insects while getting exposed to pesticides [5-7] are the consequence of the detoxification mechanism involving GST. GST catalyzes the formation of thioether conjugates between the endogenous tripeptide glutathione (GSH) and xenobiotic compounds, the major detoxification pathway in insects and human. This detoxification process sometimes creates problem when a drug is considered as a toxicant by our biological system. Overexpression is resulted in which the excessive increase of the GST level is seen. This is observed most of the time during cancer treatment. A primary cause of cancer treatment failure is an acquired or intrinsic resistance to anticancer therapies. Chemotherapeutic resistant tumor cell lines have been shown to overexpress GST isozymes. This overexpression leads to an accelerated detoxification of drug substrates and thus an acquired resistance [1]. Based on this, the specific variety of glutathione S-transferase, GST-P, is used as a marker protein during treatment of many cancers (ovarian, breast, liver, pancreas, colon, lymphomas and non-small cell lung) and high levels are linked to drug resistance even when the selected drug is not a substrate [4].

In insects increased levels of GSTs are observed when they are exposed to organochlorine, organophosphate and pyrethroid pesticides [5-8]. Thus *in-vitro* study of the GST catalyzed reaction is important not only for development of protocols for quantification of those pesticides but also to understand the molecular basis of insecticide resistance that could be an important step in developing strategies to mitigate the resistance problem.

The most commonly applied substrate for *in-vitro* study of the GST catalyzed detoxification reaction of GSH is CDNB. Both spectrophotometric [9] and

electrochemical methods have been applied for kinetic and mechanistic study of the reaction and also to quantify pesticides [10]. Compared to the spectroscopic methods, applications of electrochemical methods are not much in literature. Among the electrochemical methods two are commonly applied for the purpose. The first type involves the use of special techniques such as differential pulse voltammetry (DPV) [11] and the second type is the mediator based cyclic voltammetry [12]. To our knowledge, common electrochemical technique like the cyclic voltammetry (CV) technique has not been applied for the purpose perhaps because of the poor sensitivity that might be due to poor solubility of CDNB in phosphate buffer. GSH is soluble in phosphate buffer but CDNB is sparingly soluble in phosphate buffer. So, for a better study the GSH-CDNB reaction, an organic solvent is required. The commonly used solvent is dilute ethanol (5%). But in ethanol the intensity of the signal is found to be poor due to which special technique such as DPV or mediator based techniques have been applied to study the reaction. However such special techniques, though able to improve the signal intensity to some extent, can't help in the study of the mechanism of the reaction as well as the influence of other reactants on it due to the transient nature of the signal. Thus proper study of the influence of external reagents, particularly the pesticides, to that reaction still remains difficult. Therefore, we aim to find out alternate suitable solvents for the said reaction. As a first choice we have chosen methanol for the purpose. It has been shown in the work that though methanol is very sensitive to electro-oxidation at platinum electrode, yet it does not affect the main course reaction i.e., the GST catalyzed reaction between GSH and CDNB. The electroactive complex formed between GSH and CDNB was found to be stable for hours. Next, we aimed to study the interaction of cypermethrin, an extensively used pyrethroid class of pesticide, to the reaction. Cypermethrin in different formulations are widely used in agricultural and household pest control in different countries worldwide. Though the toxicity is relatively low in mammals, it is highly toxic for aquatic organisms and honey bees [13]. A minimal concentration of pyrethroids [0.25–1.5 mg/kg bw/day] for cypermethrin may affect immune system and central nervous system resulting in cancer and other associated disorders [14]. It has been reported in literature that many insects have the capability to develop tolerance to the pyrethroid pesticides [5]. Therefore we have chosen typical pyrethroid pesticide cypermethrin to study the influence of it on the GST catalyzed detoxification reaction of GSH.

3.2 Objectives of this chapter

- Use of simple CV technique for study of GSH-CDNB reaction.
- To observe the effect of different solvents on the activity of GST enzyme.
- Optimization of operational conditions for maximum signal output will be done by evaluating the saturated substrate concentration, maximum enzyme loading etc.
- To check the cross reactivity of different components present in the reaction mixture.
- To observe the effect of interaction between GSH-CDNB reaction with pesticides.

3.3 Experimental

3.3.1 Instrumentation

Electrochemical measurements were carried out at 32 ($\pm$ 0.05)^{0}C, using a standard electrochemical cell with three-electrode assembly. A bare Pt electrode was served as working electrode. A Pt wire was used as counter electrode and Ag/AgCl refilled with 0.1 M KCl was the reference electrode. KCl solutions were changed before each experiment. It is to be mentioned that non-aqueous Ag/Ag^+ can also be used for the purpose but due to the cost effect as well as the inconvenience in preparing the refilling Ag^+ solution, we have used the aqueous Ag/AgCl reference electrode. Cleaning of all electrodes was done before each experiment. Cyclic voltammetry (CV) measurements were performed in 0.1 M of phosphate buffer solution. Electrodes were then dipped in PB and cycled from -0.1 to 0.1 V until it acquired at a steady state baseline. UV-visible spectra were recorded to corroborate the results of CV analysis. The infrared spectra were recorded both in Mid IR and Far IR region.

3.3.2 Analysis procedure

Cyclic voltammetry and UV-visible spectroscopy were used throughout the study. The total volume of the working solution in the electrochemical cell was 3 mL and prepared by mixing 1.5 mL of 2 mM GSH in PB with 1.5 mL of 2 mM CDNB in 50% methanol, unless stated otherwise.

3.3.3 Interference study

The cross reactivity of the various components studied through CV to check whether any interference in the main course reaction was present.

3.3.4 Optimization

Saturated substrate concentration was determined through Michaelis-Menten plot and apparent Michaelis-Menten constant was obtained from the Lineweaver-Burk plot using equation 3.1.

$$\frac{1}{i} = \frac{1}{i_{max}} + \frac{k_m^{app}}{i_{max}} \frac{1}{[S]} \qquad (3.1)$$

Optimum methanol percentage was evaluated. Optimum pH for the reaction was maintained at 6.5 based on literature data [9].

3.4 Results and discussion

3.4.1 Cyclic voltammetric study of GSH-CDNB reaction in methanol

In absence of GST, the CV showed moderate intensity oxidation peak A (0.30 V, RSD 3.33%, 5.35 µA, RSD 0.37%) and the peak height remained constant with successive CV run (Figure 3.1). Another peak B appeared with onset at 0.60 V (RSD 1.66%) and peak maxima at 0.90 V (RSD 2.22%). One low intensity reduction peak (C) appeared at 0.1 V (RSD 2.94%) and disappeared after the third and successive runs. From third run onwards a low intensity oxidation peak (D) appeared at 0.05 V (RSD 1.96%) in the reverse cycle. The peak B is attributed to methanol oxidation (CO_2 formation) [16-19]. The peak A is attributed to oxidation of newly formed complex or intermediate. The reduction wave C is due to adsorption of H_2 at the platinum surface which normally occurs in the potential range from -0.23 to +0.20 V [19]. The oxidation peak at 0.05 V (actually in the region from 0.05 to 0.2 V in all the CVs, peak D) that appears in the reverse cycle is attributed to oxidation of :COH produced through dissociation of methanol (scheme 3.1). Possibility of hydrogen desorption phenomenon behind this peak is ruled out because, it did not show up in the first three runs when the adsorption waves appeared in the reverse run. And the possibility of CO oxidation is also ruled out because of the fact that CO oxidation normally occurs from 0.41 V onwards [18].

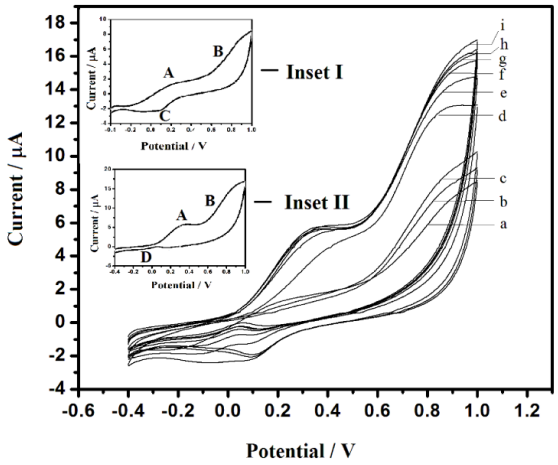

Figure 3.1. Cyclic Voltammograms recorded in a 1:1 volume mixture of 2 mM GSH in PB and 2 mM CDNB in 50% aqueous methanol at scan rate 20 mV/s after 30 minutes of mixture preparation. *Inset I*: Figure 3.1(a). *Inset II*: Figure 3.1(i).

In presence of GST the peak A became more intense (20.67 µA, RSD 0.14%), the peaks B and D remain unchanged (Figure 3.2A). The CV behavior was partially reproducible on the next day, that is, the peak A appears at same position, but the maximum intensity after several CV runs remained at almost the half height (10.45 µA, RSD 0.57%, Figure 3.2B) to that of the previous one (20.67 µA, RSD 0.14%, Figure 3.2A). This apparently indicates a two steps reaction with formation of an electroactive intermediate and the intermediate formation step is partially reversible.

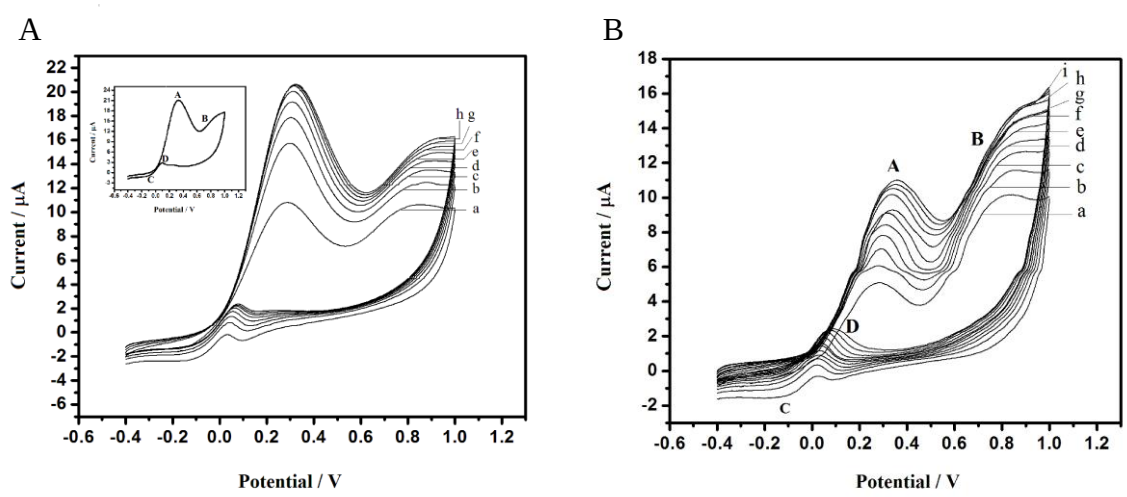

Figure 3.2. Cyclic Voltammograms recorded in a 1:1 volume mixture of 2 mM GSH in PB and 2 mM CDNB in 50% aqueous methanol and 20 µL GST (0.02 mg) at scan rate

20 mV/s. A. after 30 minutes incubation. B. in the same mixture after 24 hrs. *Inset* : Figure 3.2 A(h).

UV-visible spectroscopic study shows two absorptions, one at the 220 nm (peak M, Figure 3.3) and the other at 335 nm (peak N, Figure 3.3). The peak at 335 is due to the new complex formed, while that at 220 nm is due to methanol. The peak at 335 nm increases with time which indicates gradual formation of the complex.

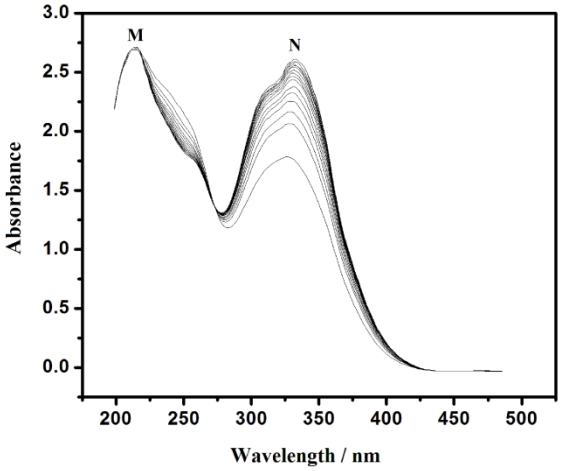

Figure 3.3. UV-visible spectra of a mixture of 2 mM each of GSH and CDNB in methanol (50%) with 20 µL GST recorded immediately after preparation.

3.4.2 Interference due to cross reactivity of the components under the applied electrochemical condition

3.4.2.1 Cross reactivity of MeOH and GSH

Shown in Figure 3.4A are the CVs of GSH and MeOH in absence of GST. The same three peaks obtained during electro-oxidation of GSH-CDNB-GST in methanol obtained in this case also, however with two distinct differences. The height of peak A is much lower than the previous case (12.98 µA, RSD 0.30%, in Figure 3.4A as compared to 20.67 µA in Figure 3.2A) and the reproducibility of the peak height (Figure 3.4B) next day was almost 100% (12.95 µA, RSD 0.23%) unlike the previous case where it was close to 50%. This infers that methanol-GSH mixture upon electro-oxidation produces intermediate complex that is completely reversible. In presence of enzyme with 30 minutes incubation, same CV pattern was obtained with slight increase in peak current

(15.20 µA, RSD 0.19%, in Figure 3.5A as compared to 12.98 µA in Figure 3.4A) indicating that enzyme catalyzes the reaction with poor catalytic performance. The enzyme catalyzed reaction on the next day was found to be reproducible again with almost same peak intensity (15.20 µA in Figure 3.5A; 14.28 µA, RSD 0.21%, in Figure 3.5B), thus, indicating the involvement of the same reaction path in absence and in presence of the enzyme.

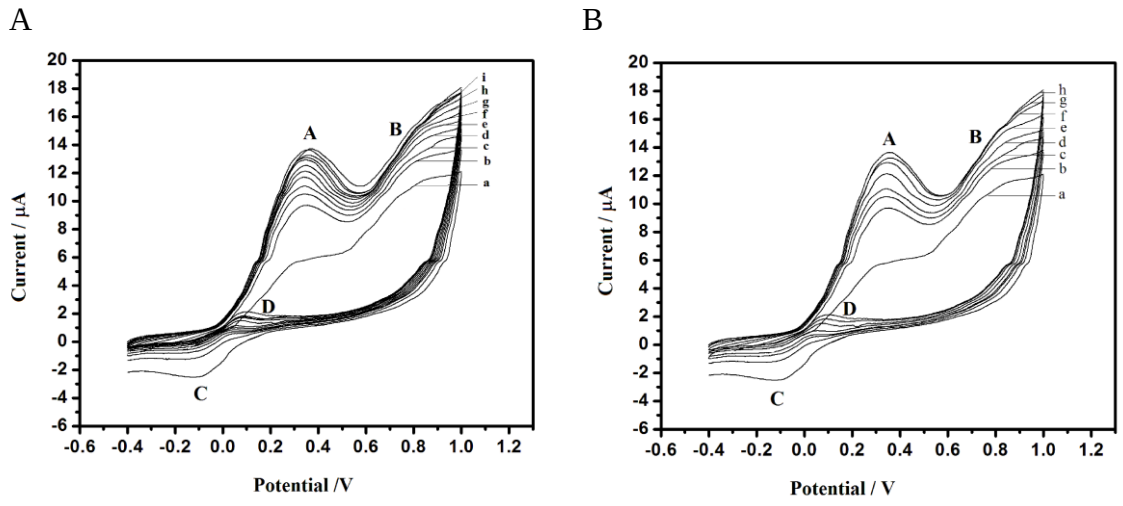

Figure 3.4. Cyclic Voltammograms recorded in a mixture of 2 mM GSH in PB and methanol with final concentration 25% at scan rate 20 mV/s. A. in a fresh mixture after 30 minutes of preparation B. in the same mixture on the next day.

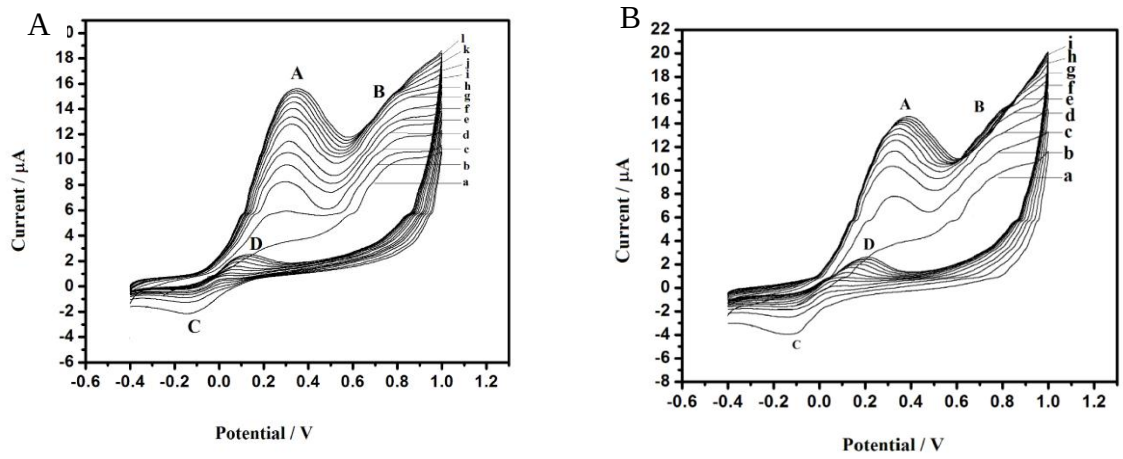

Figure 3.5. Cyclic Voltammograms recorded in a mixture of 2 mM GSH in PB and methanol (50%) with 20 µL GST at scan rate 20 mV/s. A. in a fresh mixture after 30 minutes of preparation. B. in the same mixture on the next day.

UV-visible spectra of GSH and MeOH mixture showed peak in the UV region (220 nm, peak M) but no peak in the visible region (Figure 3.6).

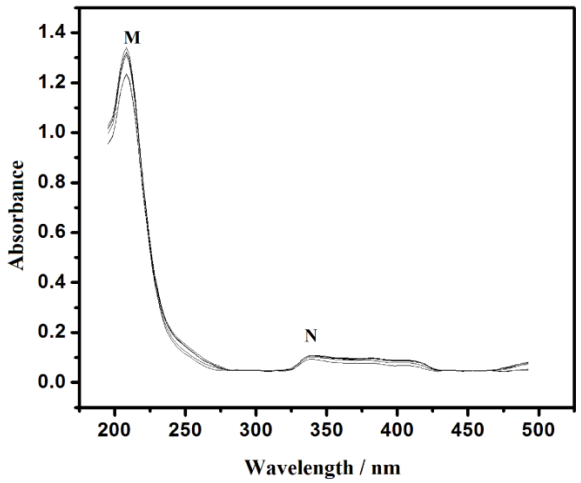

Figure 3.6. UV-visible spectra of 2 mM GSH in methanol.

To know whether the electro-oxidation has any role on the formation of UV-visible active product in the mixture of GSH, CDNB, MeOH and PB, the CV and UV experiments were performed in the same solution mixture in an alternate sequence. It was found that the CV peak maximum of peak A is affected by electrochemical disturbance when applied initially. When CV was run after completing the UV experiment the CV peak height was nearly doubled than when CV was run immediately after mixing. But the UV peak height at 335 nm reaches the same level (slowly with time) irrespective of whether disturbed electrochemically or not.

3.4.2.2 Plausible mechanism

The observed CV and UV behavior can be explained with the following reaction schemes (Schemes 3.1 and 3.2). FTIR (MIR and FIR) spectroscopic studies also corroborate this mechanism.

It is attributed that in PB solution, methanol dissociate into COH and CO^{-} in much the same way it does in strongly alkaline solution [16] (scheme 3.1). The CO^{-} thus produced interacts with GSH to produce electroactive intermediate $[GSH]^{\#}$ (scheme 3.2).

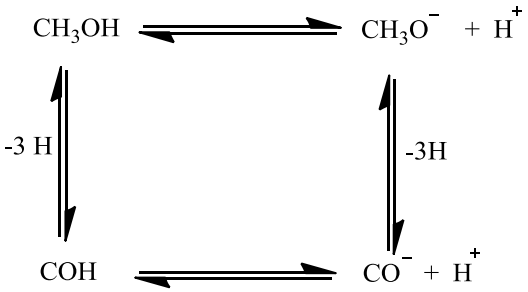

Scheme 3.1 Dissociation pathway of methanol in phosphate buffer.

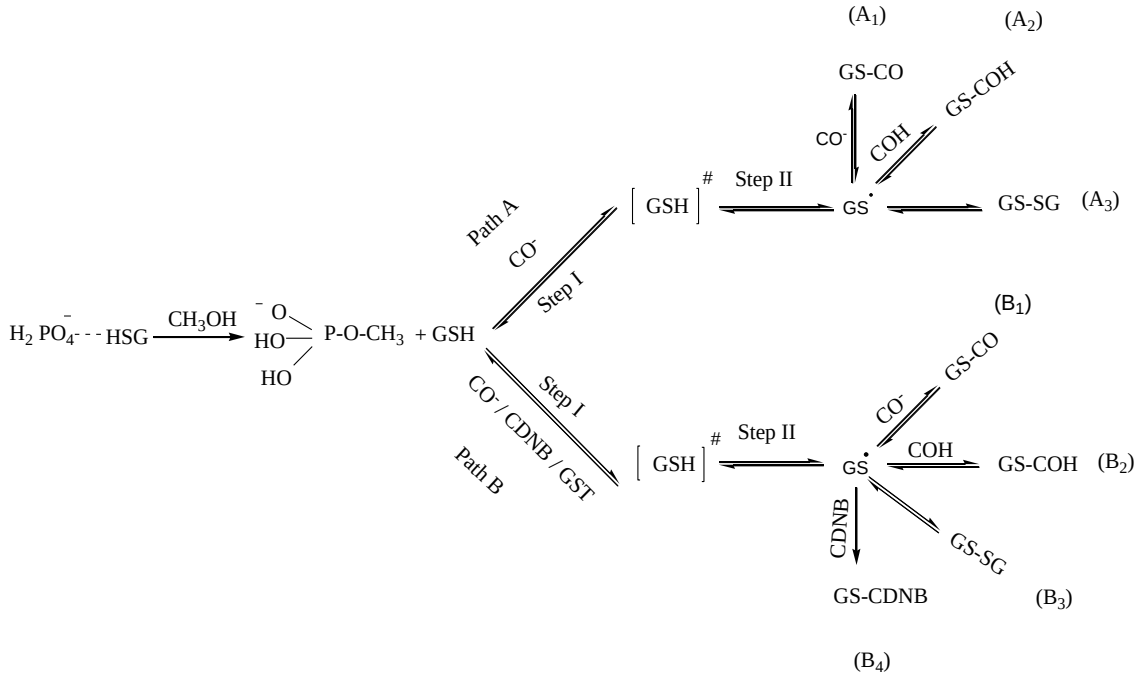

Scheme 3.2. Various possible reaction pathways in mixture of GSH, CDNB and GST in methanol.

In phosphate buffer (PB) solution GSH forms H-bonded complex with $H_2PO_4^-$ ion. Due to remaining in H-bonded state, the SH group of GSH is less reactive in phosphate buffer. In presence of methanol the situation get altered due to PB- methanol interaction and C-O-P bond formation between PB and MeOH; H-bonding network gets removed and SH groups are set free.

Path A can occur under electrochemical process in which GSH is not directly affected by the electrode potential but the CO^- formed from methanol oxidation at higher potential

(0.65V) triggers the reaction of GSH. Evidence of involvement of methanol dissociation product (CO^{-}) in the first step of path A comes from the observation that the peak at 0.30 V appears with very small magnitude initially and increases with successive run. That is, the peak height of peak A (0.30 V) is proportional to the second oxidation at higher potential (from 0. 60 V).

Path B prefers to occur under non electrochemical process. When electrochemical disturbance is applied, path A outperforms path B. The products form through paths A1, A2, B1 and B2 can occur to a lesser extent through purely non electrochemical process also. This is possible because of the fact that a certain fraction of methanol molecules remain in dissociated form (scheme 3.1) even in absence of any electrode polarization.

The peak A (at 0.30 V) is attributed to the oxidation of $[GSH]^{\#}$. The oxidation peak height of this oxidation increases with continuous CV runs up to certain time and then remains constant for more than an hour, after which it decreases slowly. So it is attributed that this oxidation involves a reversible process or a cyclic process in which the reverse step is either non-electrochemical or controlled by the second oxidation at higher potential. $[GHS]^{\#}$ formation through path B is more as compared to the same through path A. It is attributed that GST plays some role in facilitating the interaction between GSH and CO^{-}.

3.4.2.3 IR spectroscopic evidence of proposed mechanism

In phosphate buffer (PB) solution, as already stated, glutathione (GSH) forms H-bonded complex with $H_2PO_4^-$ ion due to which -SH group of GSH remain in passive state. But in presence of methanol, due to PB- MeOH interaction and C-O-P bond formation between PB and MeOH; H-bonding network gets removed and SH groups become free. This conclusion is arrived at through the observation that when GSH is added to PB, the 2086 cm^{-1} peak of PB gets masked. When methanol is added, this peak reappears and a new peak appears at 1016 cm^{-1} which was not found in the spectra of PB or MeOH. Peak at 1016 cm^{-1} is indicative of P-O-C vibration (Figure 3.7-3.8). The spectra of PB-GSH-MeOH is similar to the one of PB-MeOH. Thus IR spectra indicate presence of interaction between PB-GSH and PB-MeOH. While in the former interaction is H-bonding type, the same in the later leads to the formation of new compound with P-O-C bond.

In ethanol, due to lack of PB-ethanol interaction the PB-GSH interaction remains and as a result, the SH group becomes less sensitive to electro-oxidation. However, GST catalyzed non electrochemical reaction between GSH-CDNB still occurs leading to the UV active GS-CDNB complex (Figure 3.9).

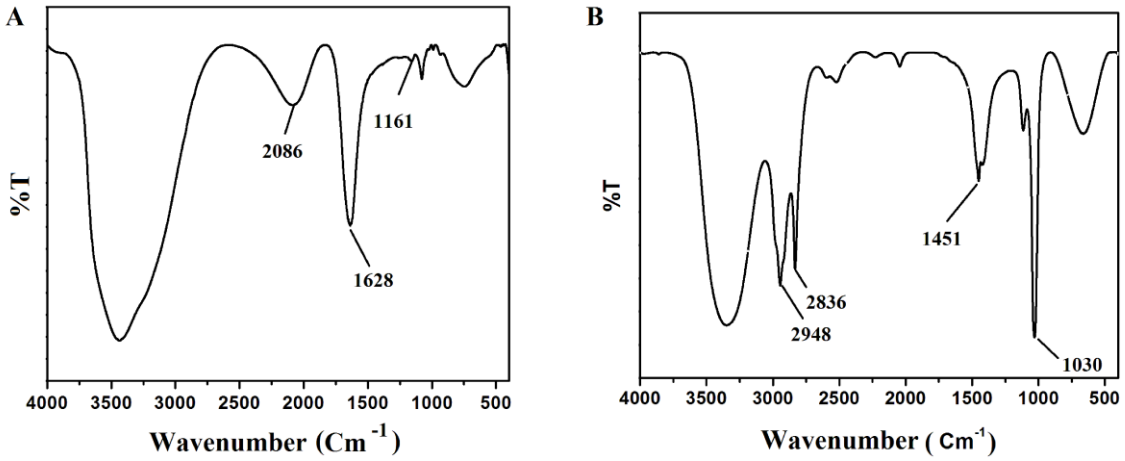

Figure 3.7. A. FTIR spectrum of phosphate buffer (PB). B. FTIR spectrum of methanol (MeOH).

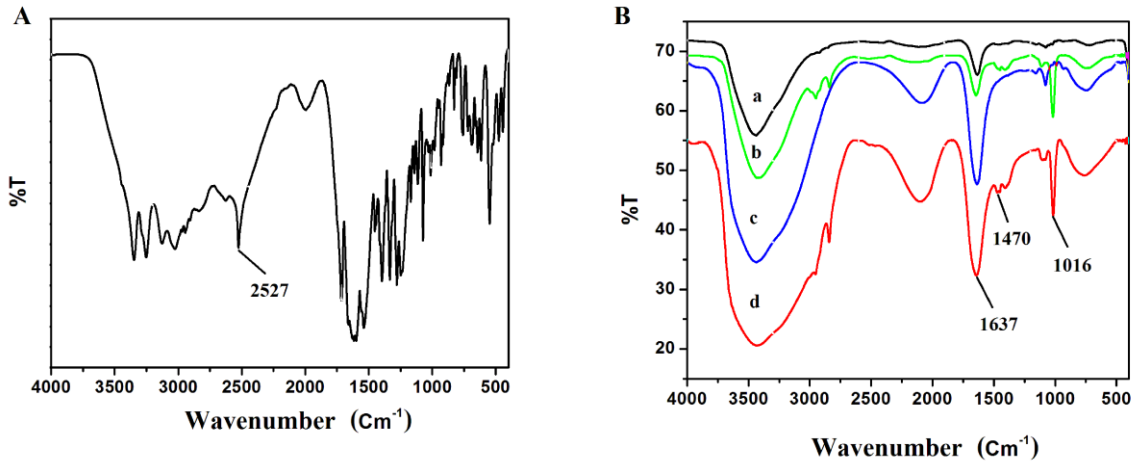

Figure 3.8 A. FTIR spectrum of solid glutathione (GSH). B. FTIR spectra of (a) GSH prepared in PB (pH 6.5) (b) GSH prepared in PB and MeOH (c) PB (d) PB and MeOH.

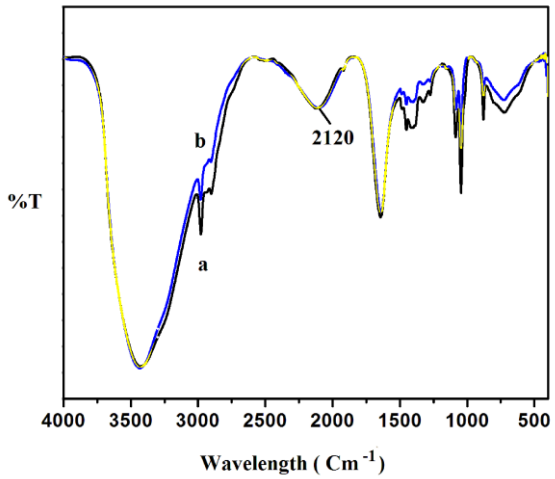

Figure 3.9. IR spectra of (a) EtOH (b) EtOH in PB (pH 6.5).

FTIR (FIR) results are shown in Figure 3.10 and 3.11. From IR spectroscopy literature it is known that peaks around 670-650 cm^{-1} are characteristic of C-S vibration and peaks around 400 cm^{-1} are characteristic of S-S vibration. In the FTIR (FIR) spectra of the reaction mixtures prominent peaks are seen in those two regions.

The two prominent peaks around 670-650 cm^{-1} indicate the formation of two different compounds with C-S bond. These are attributed to be GS-CO (670 cm^{-1}) and GS-COH (650 cm^{-1}) respectively. In absence of CDNB and GST (Figure 3.10A) the peak corresponding to GS-COH is of lower intensity than that of GS-CO in electrochemically undisturbed as well as disturbed condition. This indicates CO formation is more relative to COH in absence of CDNB and GST. Upon electrode polarization both peak increases. In presence of GST/CDNB on the other hand (Figure 3.10B), two reverse trends are seen; 1. COH formation is more than CO, both in presence and in absence of electrochemical disturbance and 2. the overall reaction (CO, COH and S-S formation) is more under electrochemically undisturbed condition than when disturbed electrochemically. The later point supports our comment that Path B is more preferred under electrochemically undisturbed condition.

While in case of GST/CDNB's presence (Path B, Figure 3.10B), GS-SG formation (470 cm^{-1}) is spontaneous, the same in their absence (Path A, Figure 3.10A) is non spontaneous and occurs under electrochemical condition only.

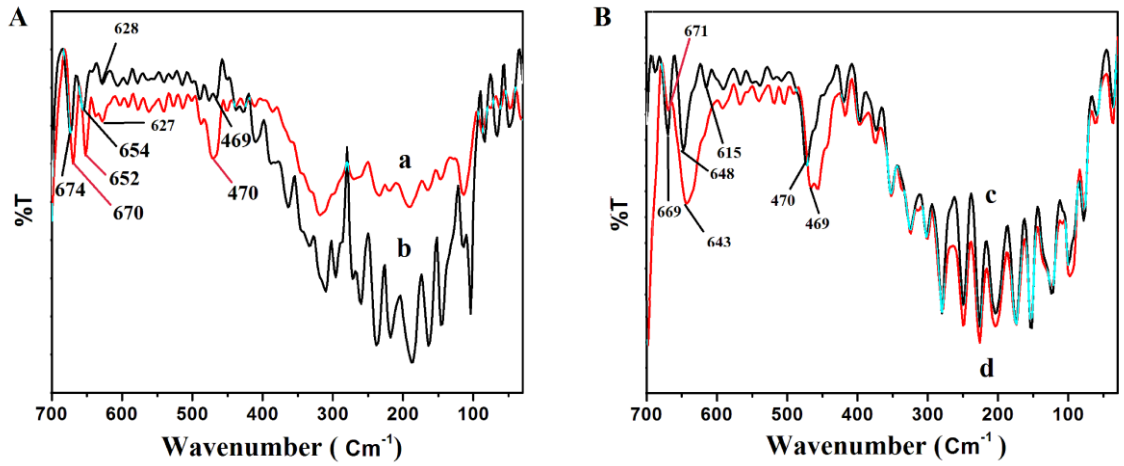

Figure 3.10. A. FTIR (FIR) plots of (a) electro oxidized solution of GSH prepared in PB and MeOH (b) solution of GSH prepared in PB and MeOH without electro-oxidation B. FIR plots of (c) electro oxidized solution of GSH, CDNB and GST mixture prepared in PB and MeOH respectively (d) solution of GSH, CDNB and GST mixture prepared in PB and MeOH respectively without electrolysis.

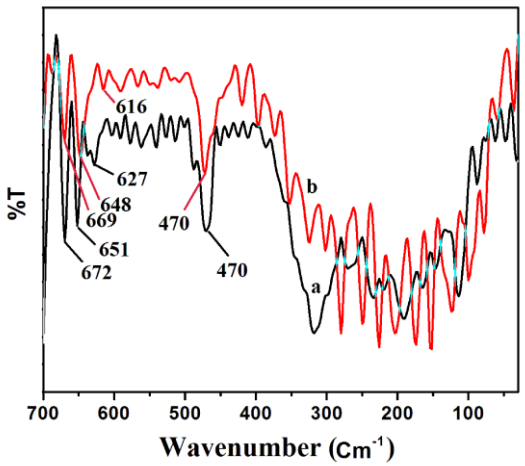

Figure 3.11. FTIR (FIR) plots of (a) electro oxidized solution of GSH prepared in PB (pH 6.5) and MeOH (b) electro oxidized solution of GSH, CDNB and GST prepared in PB and MeOH.

Figure 3.11 is the overlap of electro oxidized mixture in absence (a) and in presence (b) of CDNB/GST. The difference in 300 cm^{-1} region indicates that the effect of electrode polarization is not same in the two cases.

FTIR (MIR) spectra (Figure 3.12 -3.14) reveals that GSH-CDNB as well as GSH-GST interaction occurs through the SH bond (corresponding peak at 2330 cm^{-1}).

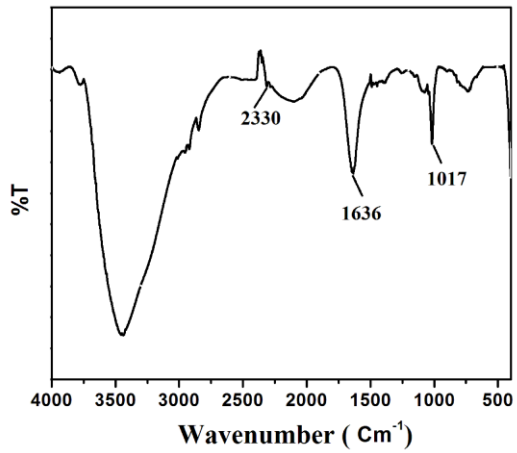

Figure 3.12. FTIR spectrum of GSH prepared in PB, MeOH and 20 µL GST enzyme.

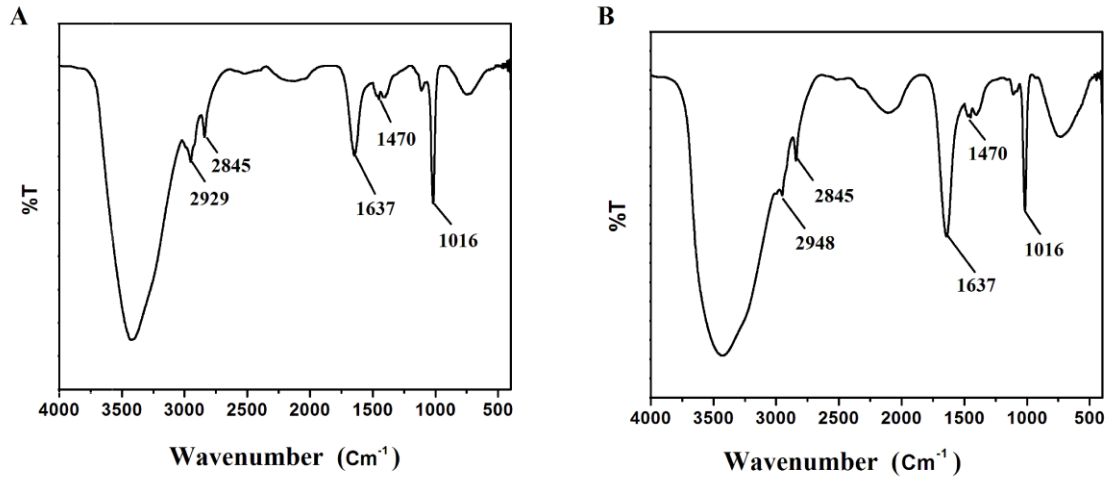

Figure 3.13. A. FTIR spectrum of GSH prepared in PB and MeOH B. Spectrum of GSH and CDNB mixture prepared in PB and MeOH.

Above three figures indicate that -SH vibration is least affected when GST is present.

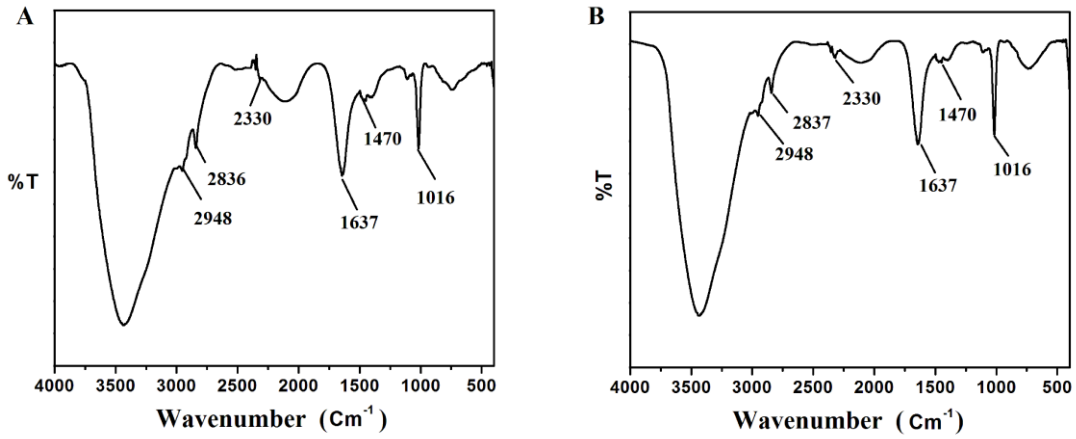

Figure 3.14. A. FTIR spectrum of GSH prepared in PB and CDNB prepared in MeOH along with 20 µL GST enzyme. B. FTIR spectrum of electro oxidized solution of GSH prepared in PB and CDNB prepared in MeOH in presence of 20 µL GST enzyme.

Above two figures indicate that -SH vibration becomes more prominent when CDNB is present in the mixture along with GST.

That the peaks around 670 - 650 cm^{-1} region are not due to C-S vibration of GS-CDNB complex is confirmed from the spectra of the same mixture recorded in ethanol (Figure 3.15). In ethanol the yellow colored complex is formed. But no peak was seen in 670-650 cm^{-1} region in the FIR. This is attributed to the higher mass of GS-CDNB as compared to GS-COH and GS-CO. The peak shows up with low intensity at lower wavenumber side (629 cm^{-1}, Figure 3.15).

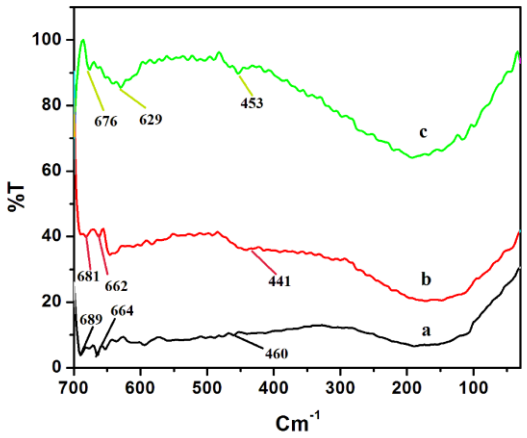

Figure 3.15. FTIR spectra of (a) GSH prepared in PB solution and that of CDNB in EtOH along with 20 µL GST recorded immediately after preparation (b) same solution

recorded after 15 min of preparation (c) after 30 min of preparation.

3.4.2.4 Cross reactivity of MeOH with PB

In Figure 3.16, curve aa/ and bb/ are the CVs of phosphate buffer methanol mixture respectively at 50% and 25% composition at scan rate 20 mV/s. With higher amount of methanol two oxidation peaks were observed peak P (0.56 V, RSD 1.78% 10.81 μA, RSD 0.27%) and Q (0.35 V, RSD 2.85%, 2.45 μA, RSD 1.22%). The oxidation peak P is attributed to oxidation of methanol (CO_2 formation step). The oxidation peak Q that shows up in the reverse cycle is due to oxidation of CO adsorbed on Pt surface [17]. Another small reduction peak R appeared at 0.02 V is attributed to reduction wave due to adsorbed hydrogen. In a dilute methanol solution the lower oxidation is not seen, the higher oxidation peak appears in a sharper pattern and gets shifted to higher potential. This shifting is attributed to creation of stronger diffusion barrier by the phosphate group created near the electrode surface due to positive electrode polarization. The low intensity reduction peak T around 0.02 V is due to charging current of H_2 adsorption.

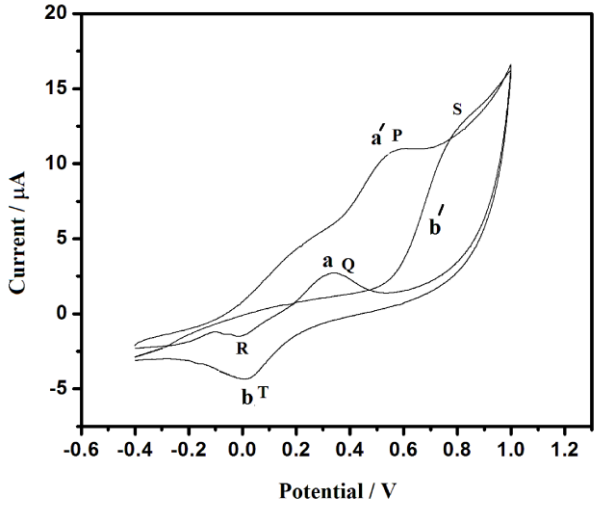

Figure 3.16. CVs at scan rate 20 mV/s of PB - MeOH mixture of composition a. 50% and b. 25%.

3.4.2.5 Cross reactivity of CDNB with MeOH

CVs of CDNB methanol mixture are shown in Figure 3.17. In methanol, two oxidation peaks were seen, one at 0.65 V (RSD 1.53%) in the forward scan and another at 0.4 V

(RSD 2.50%) in the reverse scan. These are characteristic oxidation peaks of methanol at Pt surface [16-19]. It implies that CDNB does not undergo any redox reaction under the applied experimental conditions.

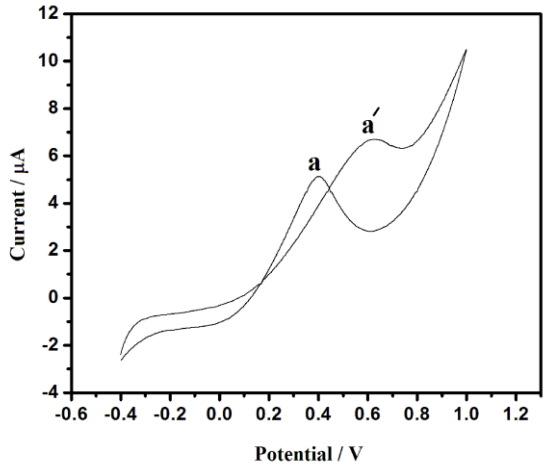

Figure 3.17. CV of CDNB in 50% aqueous methanol.

3.4.2.6 Cross reactivity of GSH with PB

CV of GSH in PB is shown in Figure 3.18. The reduction wave at a potential close to 0.10 V is probably due to reduction of oxygen adsorbed on platinum surface. A new oxidation peak of relatively lower intensity appearing from 0.60 V onwards is probably due to oxidation of some components in GSH. Due to poor intensity this oxidation gets masked by the methanol oxidation peak in the same region.

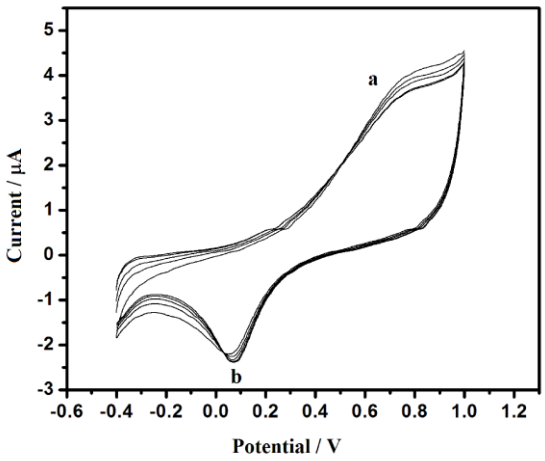

Figure 3.18. CV of reduced glutathione (GSH) in PB.

3.4.3 Optimization

Factors influencing the biosensor based on GST inhibition depends on several parameters such as the enzyme loading (in the case of irreversible inhibition), substrate concentration, time of reaction between the enzyme and the inhibitor (incubation time) and pH, thus the effect of these parameters using GST biosensors are analyzed.

3.4.3.1 Effect of GST amount

For equimolar mixture of GSH and CDNB, and for incubation time of 30 minutes, peak current was found to vary with GST concentrations. Peak current and hence the enzyme activity showed almost linear increase up to 120 μL (0.12 mg). Beyond 120 μL the reaction starts to be limited by substrate concentration (Figure 3.19). Though an amount of 0.12 mg (120 μL) of GST was found to be the maximum enzyme amount for the reaction of GSH and CDNB in 1:1 millimolar ratio, due to the preciousness of the enzyme, an amount of 20 μL (0.02 mg) was used in most of the experiments wherever possible.

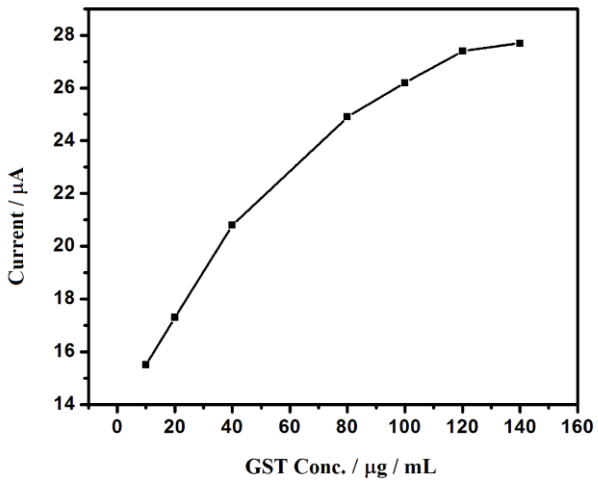

Figure 3.19. Variation of peak current of GSH-CDNB reaction (1:1 mM) in 25% methanol with GST concentration after 30 min incubation.

3.4.3.2 Apparent Michaelis-Menten constant (K_m^{app})

Effect of both GSH and CDNB concentration on the oxidation peak current was measured. A similar pattern of concentration dependency was observed indicating that both GSH and CDNB act as substrates. This is in agreement with available literature

[20]. Slightly lower current value was obtained in case of CDNB probably because of partial passivation of the Ag/AgCl reference electrode. The Michaelis–Menten plots show two different region of linear dependency. The first region is in the low concentration range from 0.5 to 2 mM and the second region is from 2 to 4 mM. Apparent Michaelis-Menten constant obtained through the Lineweaver- Burk plots (Equation 3.1) were 0.11 $mmolL^{-1}$ and 0.12 $mmolL^{-1}$ at low concentration and 1.66 $mmolL^{-1}$ and 1.91 $mmolL^{-1}$ at high concentration respectively for GSH and CDNB. The value of (K_m^{app}) reported in literature lies between 0.1 to 1 mM [21-24]. The value in the low concentration range is in good agreement with the reported values. Obtaining of the high value in the higher concentration range (2 to 4 mM) is assigned to the increasing influence of non - enzymatic reaction under high reactant density. Variation of CV peak current with GSH and CDNB concentrations is shown in Figure 3.20.

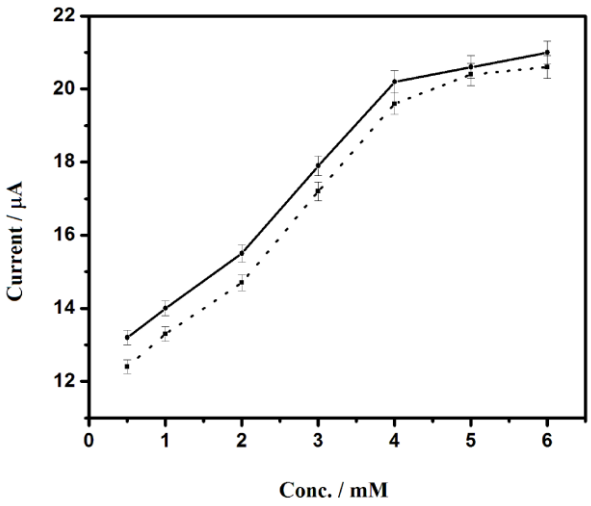

Figure 3.20. Dependency of peak current with substrate concentration when 120 µL of GST was used. Solid line for GSH concentrations, dotted line for CDNB concentrations.

3.4.3.3 Effect of incubation time

The incubation time is the reaction time of the enzyme with the inhibitor. It is possible to achieve lower detection limits using longer incubation times; in fact, the degree of the enzyme inhibition increases with the inhibition time. Usually incubation times of several minutes are chosen for pesticide detection. In fact a longer incubation time permits to achieve lower detection limits, but in these cases the analysis becomes not very fast, so

usually a compromise between a not too long measurement time and good detection limits is chosen. In our case we have chosen incubation time of 30 min for the reaction to take place.

3.4.3.4 Effect of pH

Changes in the pH of the environment can take place and alter or totally inhibit the enzyme reaction. The most favorable pH value, the point where the enzyme is most active, is known as the optimum pH. Extremely high or low pH values generally result in complete loss of activity for most enzymes. Thus, pH is also a factor in the stability of enzymes. From literature search it was found that GSTs operate most efficiently at pH 6.5.

3.4.3.5 Effect of organic solvent

The detection of different inhibitors such as pesticides and heavy metals is generally carried out in aqueous solution. However, pesticides are often characterized by low solubility in water and a high solubility in organic solvent. In general, the extraction of pesticides is carried out using organic solvent as reported in the official methods for pesticides detection, but the importance is the choice of an appropriate organic solvent to reduce the enzyme inactivation. Because, enzymes often form aggregates and denature in organic solvents. However, a few enzymes are found to be functional in organic solvents [25]. Since a solvent is necessary for solubilizing the substrates, in pesticide detection reactions, the use of high ratios of organic solvents is found to be beneficial.

3.4.3.6 Optimum methanol composition and effect of ethanol on the reaction

Effect of ethanol on the said reaction was studied using CV (Figure 3.21). When methanol was replaced with ethanol (25%) and subjected to CV analysis, no new peak other than the one from 0.6 V onwards was seen (curve e), in spite of the solution getting yellow colored. The peak from 0.6 V onwards was the same obtained in GSH-PB mixture. It indicates that the GSH-CDNB mixture does not produce any electroactive species in ethanol under the normal cyclic voltammetric condition. Effect of methanol composition on the peak intensity was studied from 5% composition onwards through CV and found that it varies linearly with composition and reaches maximum at 25%

composition. Beyond 25% composition, the increase was not significant. Thus a composition of 25% methanol was taken as the optimum methanol composition.

In ethanol, GSH electro-oxidation could not be detected by normal cyclic voltammetry (Figure 3.21). In presence of CDNB and GST an UV-visible active, yellow colored complex though formed, the reaction mixture was found to be insensitive to electro-oxidation under normal cyclic voltammetric condition.

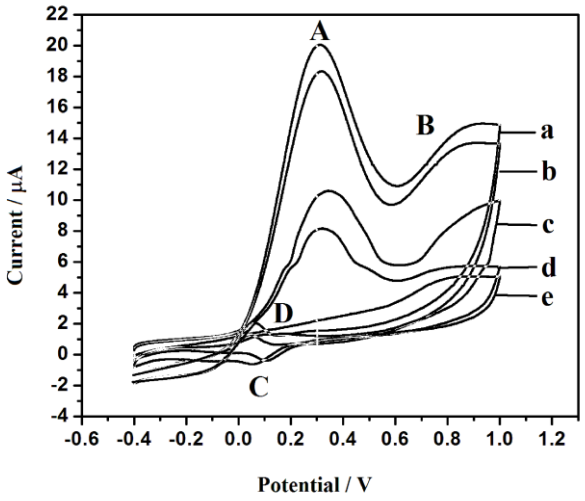

Figure 3.21. Cyclic voltammograms showing variation of peak current with methanol concentrations (a-d) and effect of ethanol (e). Reaction mixture contains 2 mM GSH, 2 mM CDNB and 20 μL GST. Methanol concentrations (a) 50% (b) 25% (c) 10% (d) 5% and ethanol concentration 25% (e).

3.4.4 Pesticides interaction study

Effect of cypermethrin on the GST catalyzed reaction between GSH and CDNB in methanol was studied. While the reaction was in progress, addition of cypermethrin suppresses the reaction to an extent proportional to cypermethrin amount. Similarly, addition of cypermethrin in the initial mixture suppresses the CV and UV-visible peak to different extent depending on the amount of cypermethrin (Figure 3.22). A 25 ppb of cypermethrin in methanol solution was sufficient for complete inhibition of the reaction in a standard 3 mL mixture of 2 mM of GSH and 2 mM of CDNB and 20 μL of the enzyme.

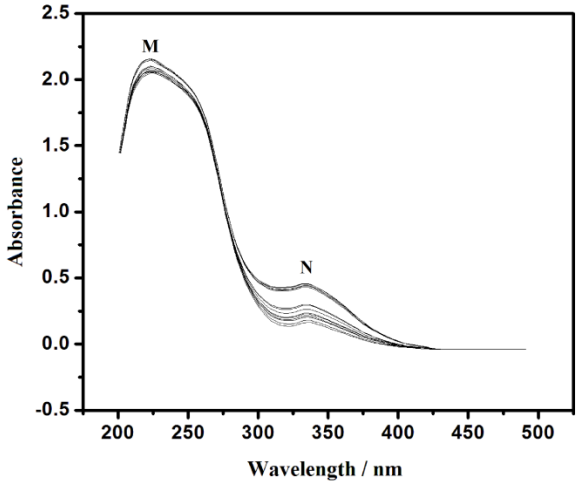

Figure 3.22. UV-visible spectra recorded in a solution mixture of GSH (1 mM), CDNB (1 mM), GST (20 μL) and PB-MeOH (25%) in presence of 25 ppb cypermethrin.

3.4.4.1 Quantification of cypermethrin

CV method was used to quantify cypermethrin. It was observed that when 25 ppb of cypermethrin was mixed initially to the solution mixture and kept for 30 min., then CV was run, the 0.3 V peak almost disappeared. Cypermethrin solutions of concentration lower than 25 ppb, when mixed in the reaction mixture, found to suppress the peak current up to different extent which was proportional to concentration of cypermethrin. Based on this observation, a calibration curve for cypermethrin was obtained by plotting percentage inhibition i.e., percentage reduction in peak current versus cypermethrin concentration up to 25 ppb and was found to be linear. Limit of detection is considered as the ppb of the pesticide required for 10% inhibition and found to be 2 ppb (Figure 3.23).

For determining the percentage inhibition two solution mixtures containing GSH-CDNB-MeOH, PB and GST of exactly same composition were prepared, one of which served as the blank. The other was treated with fixed amount of cypermethrin and the difference in CV peak current in the two were noted, which was converted to percentage inhibition.

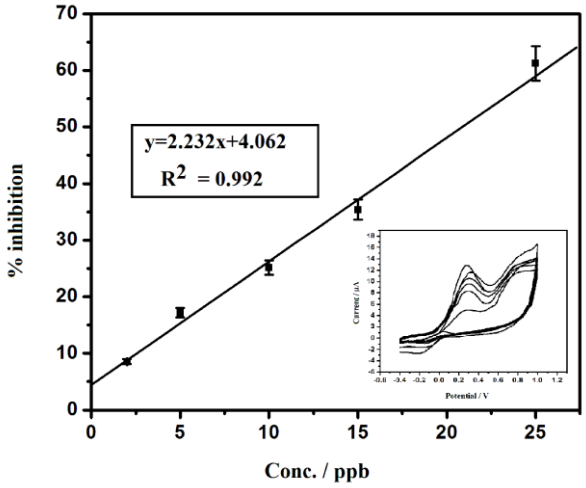

Figure 3.23. Calibration curve for cypermethrin. *Inset*: variation of CV peak current with ppb of cypermethrin.

It is obvious from the UV-visible spectroscopic study that visible spectroscopy can also be applied to quantify cypermethrin taking the GST catalyzed GSH-CDNB reaction. However, in the present work our interest was to explore the feasibility of electrochemical detection, so the spectroscopic method was not tried for.

3.4.4.2 Method validation study

For validation study, cypermethrin from spiked samples were extracted and cleaned up using modern extraction technique QuEChERS.

10 gram of chopped vegetable (tomato) was spiked with 5 mL of 60 ppb cypermethrin solution (prepared in acetonitrile) and then homogenized. 5 mL of acetonitrile was added and shaken in vortex shaker for 5 minutes. Then 4 gram of $MgSO_4.H_2O$ and 1gram of NaCl was added, shaken for 5 minutes. Then 1 g of sodium citrate dihydrate and 0.5 g of sodium hydrogen citrate sesquihydrate were added. The mixture was shaken vigorously for 10 seconds and then sonicated for 5 minutes and then centrifuged for 10 minutes at 2000 rpm. 5 mL of the supernatant was taken and treated with 125 mg of PSA (primary secondary amine) and 750 mg of $MgSO_4$ $4H_2O$, shaken for few seconds and then sonicated for 5 minute and centrifuged again. Then supernatant clean liquid was collected in 50 mL round bottom flask and evaporated to dryness at 40 ^{0}C and 200 mbar in rotary evaporator. The dry residue was reconstituted in mixture of 4 mL methanol and

1 mL dichloromethane and evaporated again to about 1 mL and then diluted to 5 mL by adding extra methanol. To 1 mL of this solution was added 1 mL each of 3 mM GSH and CDNB and 20 μL GST. Percentage inhibition in peak current calculated and pesticide amount determined with the help of the calibration curve. The whole process was repeated thrice to get triplicate results. The recovery was found to be 96.05% (RSD 1.58%).

3.5 Conclusion

Through the application of normal cyclic voltammetric method we have studied the reaction between GSH and CDNB in methanol and ethanol and shown that the reaction follows two different paths in the two solvents. Unlike the case when ethanol is used as the solvent, in methanol GSH get transformed to an electroactive intermediate state under the influence of applied electric potential. This electroactive intermediate undergoes oxidation at 0.3 V, sufficiently stable (more than one hour) and reacts with CDNB to form UV active final product. The same electroactive intermediate is also formed by non-electrochemical process in presence of CDNB and the formation is catalyzed by GST.

Influence of different components of the reaction mixture on the electrochemical response has been evaluated. Optimum GST amount, methanol concentration, saturated substrate concentration and apparent Michaelis-Menten constant for the enzymatic reaction have been determined.

We have also studied the influence of typical pyrethroid pesticide cypermethrin on the said reaction and found that cypermethrin has negative influence on the reaction. Application of the phenomena for quantifying cypermethin through cyclic voltammetric method has been demonstrated. Cypermethrin was detected down to 2 ppb by using normal cyclic voltammetric method. The quantification method has been validated through spiked sample and using QuEChERS extraction/clean up method.

References

[1] Jancova, P., Anzenbacher, P., and Anzenbacherova, E. Phase II drug metabolizing enzyme. *Biomedical Papers of the Medical Faculty of the University Palacky, Olomouc, Czechoslovakia*, 154(2):103-116, 2010.

[2] Habig, W. H., Pabst, M. J., and Jakoby, W. B. Glutathione S-Transferases- the first enzymatic step in mercapturic acid formation. *Journal of Biological Chemistry*, 249(22):7130-7139, 1974.

[3] Mcllwain, C. C., Townsend, D. M., and Tew, K. D. Glutathione *S*-transferase polymorphisms: cancer incidence and therapy. *Oncogene*, 25(11):1639-1648, 2006.

[4] Townsend, D. M. and Tew, K. D. The role of glutathione *S*-transferase in anti-cancer drug resistance. *Oncogene*, 22(47):7369-7375, 2003.

[5] Kostaropoulos, I., Papadopoulos, A. I., Metaxakis, A., Boukouvala, E., and Papadopoulou-Mourkidou, E. Glutathione S–transferase in the defense against pyrethroids in insects. *Insect Biochemistry and Molecular Biology*, 31(4-5):313-319, 2001.

[6] Pimentel, D. Environmental and Economic Costs of the Applications of Pesticides primarily in the Unites States. *Environment, Development and Sustainability*, 7(2):229-252, 2005.

[7] Lumjuan, N., Rajatileka, S., Changsom, D., Wicheer, J., Leelapat, P., Prapanthadara, L., Somboon, P., Lycett, G., and Ranson, H. The role of the *Aedesaegypti* Epsilon glutathione transferases in conferring resistance to DDT and pyrethroid insecticides. *Insect Biochemistry and Molecular Biology* , 41(3):203-209, 2011.

[8] Vontas, J. G., Enayati, A. A., Small, G. J., and Hemingway, J. A Simple Biochemical Assay for Glutathione *S*-Transferase Activity and Its Possible Field Application for Screening Glutathione *S*-Transferase-Based Insecticide Resistance. *Pesticide Biochemistry and Physiology*, 68(3):184-192, 2000.

[9] Choi, J. W., Kim, Y. K., Oh, B. K., Song, S. Y., and Lee, W. H. Optical biosensor for simultaneous detection of captan and organophosphorus compounds. *Biosensors and Bioelectronics*, 18(5-6):591-597, 2003.

[10] Choi, J. W., Kim, Y. K., Song, S. Y., Lee, I. H., and Lee, W. H. Optical biosensor consisting of glutathione-S-transferase for detection of captan. *Biosensors and Bioelectronics*, 18(12):1461-1466, 2003.

[11] Oliveira, T. I. S., Oliveira, M., Viswanathan, S., Barroso, M. F., Barreiros, L., Nunes, O. C., Rodrigues, J. A., Lima-Neto, P., Mazzetto, S. E., Morais, S., and Matos, C.D. Molinate quantification in environmental water by a glutathione-S-transferase based biosensor. *Talanta*, 106: 249-254, 2013.

[12] Sing, R. P., Kim, Y. J., Oh, B. K., and Choi, J. W. Glutathione-S-transferase based electrochemical biosensor for the detection of captan. *Electrochemistry Communications*, 11(1):181-185, 2009.

[13] Saha, S. and Kaviraj, A. Acute toxicity of synthetic pyrethroid cypermethrin to some freshwater organisms. *Bulletin of Environmental Contamination and Toxicology*, 80(1):49-52, 2008.

[14] Kaushik, A., Solanki, P. R., Ansari, A. A., Malhotra, B. D., and Ahmed, S. Iron oxide-chitosan hybrid nanobiocomposite based nucleic acid sensor for pyrethroid detection. *Biochemical Engineering Journal*, 46(2):132-140, 2009.

[15] Asensio-Ramos, M., Hernandez-Borges, J., Ravelo-Perez, L. M., and Rodriguez-Deelgado, M. A. Evaluation of a modified QuEChERS method for the extraction of pesticides from agricultural, ornamental and forestall soils. *Analytical and Bioanalytical Chemistry*, 396(6):2307-2319, 2010.

[16] Bagotzky, V. S. and Vassilev, Y. B. Mechanism of electro-oxidation of methanol on the platinum electrode. *Electrochimica Acta*, 12(9):1323-1343, 1967.

[17] Chetty, R., Xia, W., Kundu, S., Bron, M., Reinecke, T., Schuhmann, W., and Muhler, M. Effect of Reduction Temperature on the Preparation and Characterization of Pt-Ru Nanoparticles on Multiwalled Carbon Nanotubes. *Langmuir*, 25(6):3853-3860, 2009.

[18] Herrero, E., Chrzanowski, W., and Wieckowski, A. Dual Path Mechanism in Methanol Electro-oxidation on a Platinum Electrode. *The Journal of Physical Chemistry*, 99(25):10423-10424, 1995.

[19] Zhou, C., Wang, H., Peng, F., Liang, J., Yu, H., and Yang, J. MnO_2/CNT Supported Pt and Pt-Ru Nanocatalysts for Direct Methanol Fuel Cells. *Langmuir*, 25(13):7711-7717, 2009.

[20] Enache, T. A. and Oliveira-Brett, A. M. Electrochemical evaluation of glutathione S-transferase kinetic parameters. *Bioelectrochemistry*, 101:46-51, 2015.

[21] Adams, P. A. and Sikakana, C. N. T. Factors affecting the inactivation of human placental glutathione *S*-transferase π: The kinetic mechanism and pH-dependence of solvational and 1-chloro-2,4-dinitrobenzene-mediated inactivation of the enzyme. *Biochemical Pharmacology*, 39(12):1883-1889, 1990.

[22] Grammou, A., Papadimitriou, C., Samaras, P., Vasara, E., and Papadopoulos, A. I. Effect of municipal waste water effluent upon the expression of Glutathione S-transferase isoenzymes of brine shrimp *Artemia. Chemosphere*, 84(1):105-109, 2011.

[23] Valles, S. M., Perera, O. P., and Strong, C. A. Purification, biochemical characterization, and cDNA cloning of a glutathione *S*-transferase from the red imported fire ant, *Solenopsisinvicta. Insect Biochemistry and Molecular Biology*, 33(10):981-988, 2003.

[24] Zibaee, I., Bandani, A. R., Haghani, S., and Zibaee, A. Partial characterization of Glutathione S-Transferase in two populations of the sunn pest, *eurygasterintegriceps* puton (Heteroptera: Scutellaridae). *Munis Entomology and Zoology*, 4:492-499, 2009.